

Synthesis of eggshell cobalt catalysts by molten salt impregnation techniques

Stuart L. Soled^a, Joseph E. Baumgartner^a Sebastian C. Reyes^a, and Enrique Iglesia^b

^aCorporate Research Laboratories, Exxon Research and Engineering Co. Route 22 East, Annandale, NJ 08801

^bDepartment of Chemical Engineering, University of California, Berkeley, CA 94720

Fischer-Tropsch synthesis catalysts with the active cobalt component preferentially located near the outer surface of support pellets were prepared by impregnation with molten cobalt nitrate. This synthesis procedure and the slow reduction of the impregnated nitrate to Co metal led to relatively high metal dispersions (0.05-0.1) at the high Co concentrations (40-50% wt.) present within the shell region. The eggshell thickness is determined by the melt viscosity and by the contact time between the melt and the porous pellet and agrees well with values predicted by imbibition models using measurements of liquid and support properties. The resulting eggshell catalysts introduce intermediate levels of transport restrictions, which lead to optimum C₅₊ yields in the Fischer-Tropsch synthesis.

I. INTRODUCTION

Whereas changes in Co or Ru dispersion or in the type of metal oxide support (e.g., SiO₂, Al₂O₃, etc.) have only a weak effect on Fischer-Tropsch (FT) synthesis turnover rates, diffusional constraints can dramatically alter apparent turnover rates and selectivities [1-6]. Transport restrictions become increasingly important when large catalyst pellets (1-3mm) are used in packed-bed reactors in order to avoid substantial pressure drops. As previously shown by Iglesia et al. [4-6], at typical FT synthesis conditions, two types of reaction-diffusion couplings occur: (a) diffusion-limited product removal from catalyst pellets and (b) diffusion-limited reactant arrival at catalytic sites. In the first regime, diffusion-enhanced readsorption of α -olefins leads to higher product molecular weight and paraffin content as pellet size or active site density increase. In the second regime, catalyst pellets become depleted of CO, which favors formation of lighter products and decreases the desirable C₅₊ selectivity.

Growing chains that desorb as olefins can readsorb and initiate chain growth, leading to desirable higher molecular weight products. As pellet size, site density or olefin carbon number increase, the probability of readsorption increases. With increasing transport restrictions, the catalytic sites are exposed to higher effective H₂/CO ratios, which produce undesirable lower molecular weight products. Intermediate levels of transport restrictions lead to optimum product distributions.

We can modify the extent of transport limitations by manipulating the thickness of the active layer and the volumetric density of active sites during catalyst synthesis. The benefits of non-uniform intrapellet site distributions have been previously described for many catalytic reactions, including the Fischer-Tropsch synthesis [7-15]. Here, we report on the preparation of large SiO₂ pellets with uniform and eggshell Co distributions. The eggshell catalysts contain Co near the outer support surface when prepared by impregnating 2 mm silica spheres with molten cobalt nitrate. The local cobalt content approaches 50% wt. in a 0.1mm external shell; yet, we can obtain relatively high Co dispersions (0.05-0.10) by directly reducing the nitrate precursor at a slow heating rate.

2. EXPERIMENTAL

In order to study the catalyst preparation process, we measured capillary imbibition rates of four different liquids on individual SiO₂ spheres (Shell S980B, 260 m²g⁻¹, calcined at 873K) that were glued with an epoxy resin to the ends of wooden applicator sticks. A standard aqueous solution (A, Table 1) contained 0.5 g Co nitrate/cm³ H₂O. A melt of cobalt nitrate held at temperatures between (333 and 348K) provided a higher viscosity (31-48 cp) liquid. We prepared an aqueous cobalt nitrate solution (B) with similar viscosity to the cobalt nitrate melt by adding 1.0% wt. hydroxyethylcellulose to solution (A). A fourth solution (C), with low cobalt content, contained 0.01 g Co nitrate/cm³ of H₂O.

In order to characterize solution properties, viscosity and surface tensions were measured with a Nametre vibrating sphere viscometer and a Kruss K-10 tensiometer (ring method), respectively. The individual silica spheres were immersed in the four liquids for periods of 2,4,8,16,32, and 48 s. We then removed any excess liquid from the spheres, dried them for 0.5 h, and then calcined them in air at 623 K for 0.25 h. This treatment converted the nitrate to Co₃O₄, which provided sharper contrast in optical microscopy measurements. These immersion experiments were also repeated using heated (383K) and cooled (263K) silica spheres. Each data point was averaged from measurements on 10 individual spheres.

Several cobalt catalysts were prepared on both powder and large particle carriers for testing in FT reactors. SiO₂ powders (Davison 62, W. R. Grace Co., 280 m²g⁻¹, calcined 873 K, 0.143 mm average pellet diameter) were slurried with a cobalt nitrate (Co(NO₃)₂ · 6H₂O, Alfa)/acetone solution and the excess solvent was evaporated. Both uniformly impregnated and eggshell pellets were prepared. The uniform pellets were prepared by incipient wetness impregnation of silica spheres (either Shell S980G: 115 m²g⁻¹, 2.2 mm pellet diameter, or Shell S980B: 1.7 mm pellet diameter, 260 m²g⁻¹; both calcined at 873 K for 16 h) with aqueous Co nitrate solutions. Ground samples of these pellets were obtained by crushing and separated into different size ranges (0.13 to 0.86 mm).

The eggshell catalysts were prepared by imbibition with high viscosity (~ 40cp) cobalt nitrate melts. Molten Co nitrate (50 g, melting point ~323 K) at 348-363 K was poured uniformly over a 2-3 cm bed of SiO₂ spheres (2-3 cm bed height, Shell S980G, 12.5g) that in turn was placed on top of a 15-20 mm layer of 6 mm non-porous glass beads held in a glass funnel (5.5 cm diameter). As the cobalt nitrate melt was added, the bed was stirred with a glass rod, and the molten nitrate was removed by vacuum filtration in order to limit contact times to 2-4 s. For comparison, samples were also prepared using this controlled contact time technique but with a room temperature aqueous Co nitrate solution (100 cm³ Solution A,

Table 1) instead of the nitrate melt.

All catalysts were directly reduced in flowing hydrogen. The samples were heated at 6-12 K h⁻¹ from room temperature to 693-723 K and held at this temperature for 4-16 h. The samples were then passivated with a dilute oxygen stream (1% O₂/He) at room temperature before use. All catalysts were characterized by x-ray diffraction, hydrogen chemisorption, nitrogen physisorption, and optical microscopy. Co was analyzed by atomic absorption or by gravimetric measurements during reduction and oxidation cycles. Cobalt dispersion was measured by hydrogen chemisorption at 373 K assuming a 1:1 H:Co surface stoichiometry (1).

The reduced and passivated catalysts were mixed with fine quartz powder (0.1-0.2 mm diameter) to insure isothermal operation and avoid bypassing, introduced into packed-bed reactors, and re-reduced in flowing H₂ at 623-723 K for 2-4 h. After cooling to 473 K, the catalyst was exposed to H₂ and CO reactants (H₂/CO=2/1), temperatures were maintained at 473 K and pressures at 2000 kPa. Data were collected after reaching steady state (24-36 hours), and the products were analyzed with gas chromatography and mass spectroscopy [5]. Selectivities are reported as the percentage of reacted CO that appears as a given product.

3. RESULTS AND DISCUSSION

3.1. Liquid imbibition into porous SiO₂ pellets

The imbibition of a liquid into a sphere depends on both solution properties (viscosity and surface tension) and solid properties (pore radius, pore tortuosity, and contact angle). Washburn [16] showed for a liquid partially penetrating a sphere through cylindrical capillaries, the fractional penetration depth was equal to:

$$\zeta = \Omega \cdot t^{1/2} \quad (1)$$

where

$$\Omega = [1/(\tau \cdot R_0^2) \cdot \gamma \cdot r_p \cdot \cos(\theta)/(2 \cdot \mu)]^{1/2}$$

and μ is the liquid viscosity, γ the surface tension, r_p the pore radius, τ the tortuosity of the pore structure, R_0 the pellet radius, and θ the contact angle between the liquid and the support surface.

In the initial experiments, a given support pellet was immersed into molten cobalt nitrate and Solutions A, B and C for varying periods of time. The fractional penetration depth should depend on both viscosity and surface tension (assuming no change in contact angle). Table 1 shows that the surface tension of nitrate solutions, of solutions viscified with hydroxyethylcellulose (HEC), and of nitrate melts are similar, so that penetration depth should depend only on solution viscosity. Figure 2 shows the liquid penetration depths plotted against $t^{1/2}$. As suggested by Washburn's Eqn. (1), a plot of ζ vs. $t^{1/2}$ gives a straight line with slope Ω . We assumed perfect wetting of solid surfaces by the liquid ($\theta=0$) and a pellet tortuosity value of 1.8. Table 2 shows the slopes from Figure 2 and those calculated from Eqn. (2) using measured pore structure and solution properties.

Surprisingly, nitrate melts (at 333 K) penetrate into silica spheres (2.7 mm diameter, 210 m²g⁻¹) more slowly than nitrate solutions of similar viscosity and surface tension at room

Table 1
Properties of impregnating nitrate solutions and melts.

Impregnating Liquid	Hydroxy ethylcellulose (wt%)	Viscosity (μ ; cp)	Surface Tension (γ , dynes cm^{-1})
Solution A ⁽¹⁾	0	3.2 (298K)	65.6
Solution B ⁽¹⁾	1.0	45 (298K)	66.4
melt	0	48 (333K)	--
melt	0	31 (348K)	66.2
Solution C ⁽²⁾	0	0.93 (298K)	66.9
Water	0	0.92 (295K)	70.6

(1) 0.5 g Co nitrate/cm³ H₂O

(2) 0.01 g Co nitrate/cm³ H₂O

temperature (Solution B, Figure 1,ii and iii; curves C and B, Figure 2). As expected, both liquids penetrate silica spheres slower than aqueous nitrate solutions without HEC (Figure 1,i and curve A in Figure 2). In order to determine if the slow penetration of the melt resulted from cooling and solidification as it contacted the spheres, we measured imbibition rates into silica spheres heated (383K; curve C" in Figure 2) or cooled (263K; curve C' in Figure 2) before immersion. In both cases the behavior resembles that of spheres held at room temperature. The unexpected rapid penetration of the 1%HEC/cobalt nitrate solution suggests that the solution viscosity within a support pore is much lower than in the bulk liquid. Pyrolyzing 1% HEC impregnated (cobalt-free) pellets at 673K in N₂ and examining the pellets via EDS showed that most of the HEC additive remains on the external pellet surfaces and is therefore ineffective in retarding imbibition within intrapellet pores. The agreement between theoretical and experimental penetration values is excellent for nitrate melts and solutions; experimental penetration rates differ significantly from theoretical predictions only for viscosified nitrate solutions, where surface retention of HEC renders the use of bulk viscosity in the Washburn model inappropriate.

In order to produce large quantities of eggshell pellets for catalytic testing, we developed a vacuum filtration technique in which an excess of molten cobalt nitrate was poured over silica pellets held in a vacuum funnel and then filtered quickly. The vacuum filtration technique controls the liquid-pellet contact time while the high nitrate melt viscosity slows pellet imbibition during the contacting. Fig. 3,ii shows silica spheres (2.2 mm, 115 m²g⁻¹) impregnated with molten Co nitrate (348-363 K) for 2-4 s using vacuum filtration to remove the excess melt. The pellets contain 10-13% wt. cobalt and with 75% of the SiO₂ pellet volume void of cobalt, the local Co content in the shell is close to 50% wt. When the same technique was applied to aqueous Co nitrate solutions (Solution A, Table 1) in place of melts, the impregnating solution completely penetrated the silica spheres (Figure 3,i)

3.2. Cobalt dispersion and crystallite size

Cobalt tends to form large crystallites on metal oxide supports. Cobalt dispersion, defined as the fraction of the metal atoms residing at crystallite surfaces, rarely exceeds 0.1, except when using organometallic precursors [5]. These precursor often leave carbonaceous residues and the resulting small crystallites tend to re-oxidize during FT synthesis.

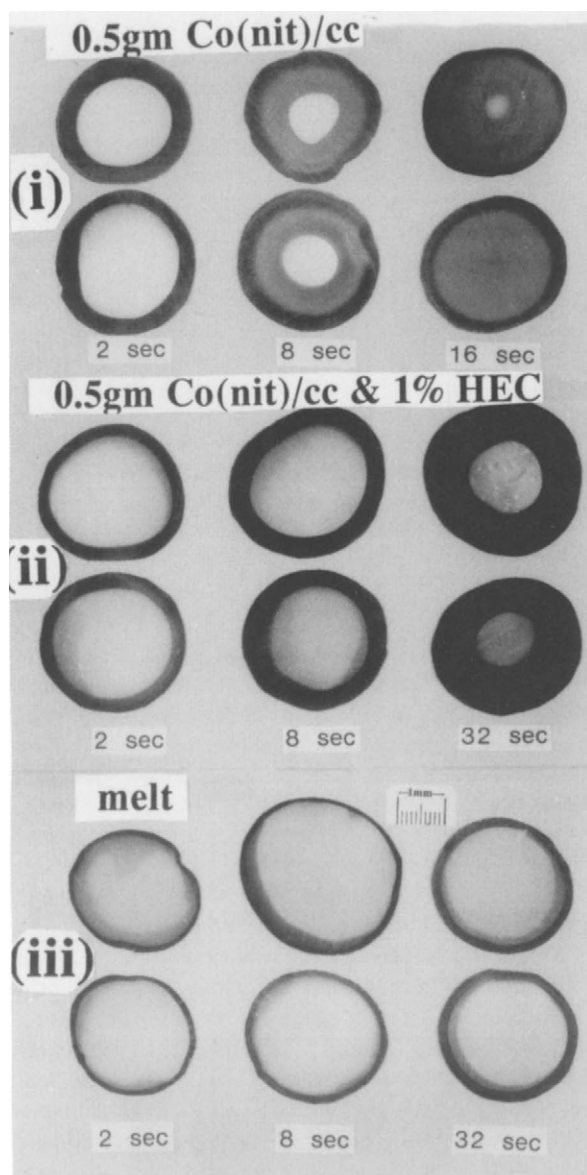


Figure 1. Optical micrographs of silica pellets individually immersed in solutions or melt:
 (i) solution A, 0.5 g Co nitrate/cm³ H₂O
 (ii) solution B, 0.5 g Co nitrate/cm³ H₂O & 1% wt. hydroxyethylcellulose
 (iii) cobalt nitrate melt (333K)

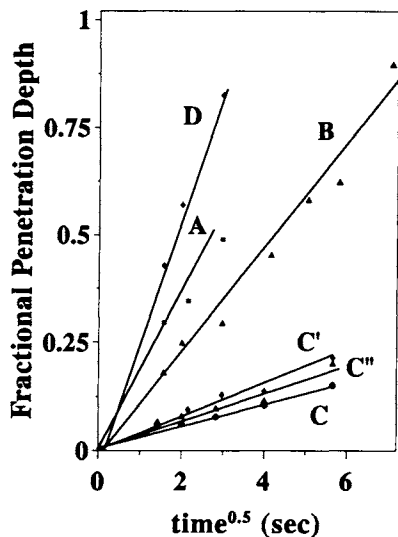


Figure 2. Effect of Impregnating Solution on Liquid Penetration Depth (SiO_2 : 210 m^2/g ; 2.7mm diameter);

- A: solution A; 0.5gm Co nitrate/ cm^3 H_2O
- B: solution B; 0.5gm Co nitrate/ cm^3 H_2O & 1 % HEC
- C: nitrate melt, SiO_2 at 298K;
- C': nitrate melt, SiO_2 at 273K;
- C'': nitrate melt, SiO_2 at 383K;
- D: solution C; 0.01gm Co nitrate/ cm^3 H_2O

Table 2

Liquid penetration rates. Comparison of experimental values and model predictions.

Impregnating Liquid/Solution	Liquid Temperature (K)	Sphere Diameter ($2 \cdot R_0$, cm)	Average Pore Radius (r_p /nm)	Slope (from Fig. 2)	Slope (from eqn 2)
A	298	0.27	8.5	0.18	0.16
B	298	0.27	8.5	0.12	0.045
B	298	0.22	16.0	0.12	0.075
melt	333	0.27	8.5	0.028	0.042
melt	333	0.22	16.0	0.085	0.074
melt	348	0.27	8.5	0.035	0.052
(silica at 383K)					
melt	348	0.27	8.5	0.041	0.052
(silica at 263K)					
C	298	0.27	8.5	0.29	0.31

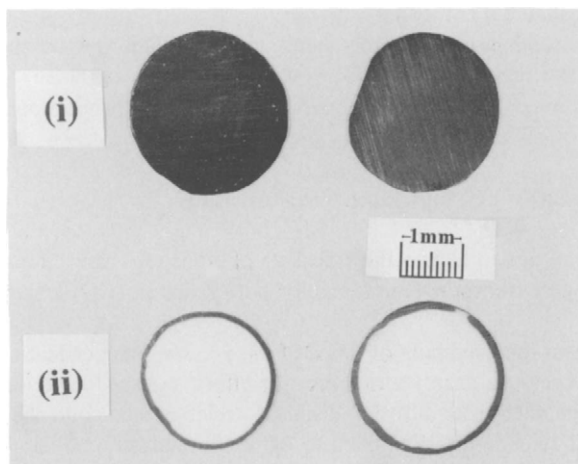


Figure 3. Optical Micrographs of silica pellets impregnated using the vacuum filtration procedure: (i) solution A, 0.5 g Co nitrate/cm³ H₂O (ii) impregnation of melt.

Sintering occurs more readily at high metal loadings. As a result, we expect cobalt dispersions to be very low at the locally high Co concentrations in our eggshell catalysts. We have found, however, that slow direct reduction of nitrate precursors leads to Co dispersions in eggshell catalysts that are similar to those obtained by conventional pretreatments in uniformly impregnated pellets, where local Co levels are significantly lower.

High dispersions in eggshell catalysts require that we reduce the nitrate salts directly in flowing dihydrogen while ramping the temperature slowly (<12 K h⁻¹) and that we avoid any intermediate calcination step. When we calcine a sample at 623 K for 3h and then reduce in hydrogen by heating the sample to 723 K at 240 K h⁻¹, the cobalt dispersion is 2.8% (33 nm average crystallite size). Reducing nitrate precursors directly in hydrogen at similar conditions without an intermediate calcination increases the metal dispersion to 4.2 % (23 nm average diameter). When we reduce the nitrate directly but at a heating rate of 12 K h⁻¹, the cobalt dispersion increases to 5.5% (17 nm average crystallite diameter).

These results suggest that extensive sintering occurs during uncontrolled calcination of nitrate precursors leading to agglomerated oxide particles. Sintering also occurs during uncontrolled reduction of these nitrate precursors, possibly as a result of local exotherms or of the presence of high concentration of reduction products (H₂O, NO_x, and nitric acid). The combination of melt impregnation synthesis techniques with slow reduction of nitrate precursors leads to well-defined eggshell regions within which small cobalt crystallites (10-20 nm) are formed at high local Co concentrations (40-50 % wt.). The resulting catalysts retain the high volumetric productivity of uniformly impregnated small pellets, while introducing transport restrictions that lead to optimum yields of desired C₅+ products.

3.3. Optimum C_5+ selectivity on eggshell Co catalysts

Extensive catalytic tests on small and large uniformly impregnated pellets and on the eggshell catalysts of this study show that maximum C_5+ selectivities are obtained at intermediate levels of transport restrictions (Figure 4). The parameter χ , and is proportional to:

$$\chi \propto (\text{characteristic diffusion length})^2 \cdot (\text{volumetric active site density})$$

describes how catalyst structural properties influence the intensity of transport restrictions. Increasing values of χ reflect more severe transport limitations for both reactant (CO) arrival and product (olefin) removal.

Eggshell catalysts can be placed near the maximum of this C_5+ vs. χ curve independent of the pellet diameter required to avoid pressure drop restrictions. In effect, eggshell catalysts decouple the pellet diameter from the characteristic diffusion distance, which is then controlled independently by varying the eggshell thickness. Within these eggshell catalysts, moderate transport restrictions retard the removal of reactive olefins, which then readsorb and initiate surface chains leading to higher molecular weight products. Transport restrictions, however, are not sufficiently severe to introduce CO concentration gradients that reduce catalyst effectiveness and lead to undesirable lighter hydrocarbons.

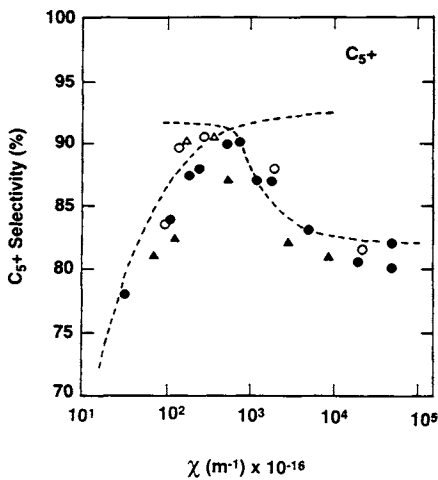


Fig. 4. C_5+ Selectivity as a function of increasing transport limitations at 473 K, $H_2/CO=2.1$, 2000 KPa and 50-60% CO conversion. O represent eggshell catalysts while ● are powder catalysts and ▲ are even pellets of different diameter.

4. ACKNOWLEDGMENTS

We thank Dr. Rocco A. Fiato for many helpful discussions and Ms. Hilda Vroman and Mr. Bruce DeRites for the synthesis, characterization, and catalytic evaluation of some of these materials. We also thank Dr. Eric Herbolzheimer and Ms. Dee Redd for the viscosity and surface tension measurements.

REFERENCES

1. E. Iglesia, S. L. Soled, and R. A. Fiato, *J. Catal.*, 137 (1992) 212
2. E. Iglesia, S. C. Reyes, and R. J. Madon, *J. Catal.*, 129 (1991) 238 .
3. R. J. Madon, S. C. Reyes, and E. Iglesia., *J. Phys. Chem.*, 95 (1991) 7795.
4. E. Iglesia, S. C. Reyes, and S. L. Soled, in "Computer-Aided Design of Catalysts and Reactors" (E. R. Becker and C. J. Pereira, eds.), p. 199, Marcel Dekker, New York, 1993.
5. E. Iglesia, S. C. Reyes, R. J. Madon, and S. L. Soled, in "Advances in Catalysis and Related Subjects" (D. D. Eley, H. Pines, and P. B. Weisz, eds.) vol 39, p. 239. Academic Press, New York, 1993.
6. R. J. Madon, S. C. Reyes, S.C., and E. Iglesia, in "Selectivity in Catalysis", ACS Symposium Series (S. L. Suib, and M. E. Davis, eds.) 1992.
7. R. W. Maatman and C. D. Prater, *Ind. Eng. Chem.*, 49 (1957) 253 .
8. W. E. Corbett and D. Luss, *Chem. Eng. Sci.*, 29 (1974) 1473 .
9. C. J. Pereira, G. Kim, and L. L. Hegedus, *Catal. Rev. Sci. Eng.*, 26 (1984) 583 ; J. E. Summers and L. L. Hegedus, *J. Catal.*, 51, (1978) 185.
10. R. S. Dixit and L. L. Tavlarides, *Chem. Eng. Sci.*, 37, (1982) 59; *Ind. Eng. Chem. Proc. Des. Dev.*, 22 (1983) 1
11. R. C. Everson, E. T. Woodburn, and A. R. M. Kirk, *J. Catal.*, 53 (1978) 186.
12. A. Niemark, A. Khelfez, and V. Fenelonov, *Ind. Eng. Chem. Prod. Res. Dev.*, 20 (1981) 439.
13. M. F. M. Post and S. T. Sie, *Eur. Pat. Appl.* 174,696 (1985).
14. W. A. van Erp, J. M. Nanne, and M. F. M. Post, *Eur. Pat. Appl.* 178,008 (1985).
15. R. S. Sapienza, M. J. Sansone, W. Anthony, and R. Slegeir, GB Patent 2,104,405A (1983)
16. E. Washburn, *Phys. Rev.*, 17 (1921) 273.